Journal of Nuclear Materials 390–391 (2009) 140–143

Contents lists available at ScienceDirect

Journal of Nuclear Materials

journal homepage: www.elsevier.com/locate/jnucmat

Carbon dust formation in a cold plasma from cathode sputtering

C. Arnas [a,*], A. Mouberi [a], K. Hassouni [b], A. Michau [b], G. Lombardi [b], X. Bonnin [b], F. Bénédic [b], B. Pégourié [c]

[a] Laboratoire de Physique des Interactions Ioniques et Moléculaires (PIIM), Faculté des Sciences de St. Jérôme, Université de Provence, Case 321, F-13397 Marseille cedex 20, France
[b] Laboratoire d'Ingénierie des Matériaux et des Hautes Pression (LIMHP), Université Paris 13, 93430 Villetaneuse, France
[c] Association Euratom-CEA, CEA Cadarache, CEA/DSM/IRFM, 13108 St. Paul Lez Durance, France

ARTICLE INFO

PACS:
52.27.Lw
52.40.Kh
52.65.−y
81.05.Uw

ABSTRACT

Nanoparticles are produced in argon glow plasmas where carbon is introduced by sputtering of a graphite cathode. A scaling law of growth is reported on as a function of the discharge time. Two successive stages of growth of concomitant agglomeration and carbon deposition are observed, followed by a final stage of growth by carbon deposition. A model of formation of molecular precursors by coagulation of neutral clusters on the one hand and of neutral-negative clusters on the other hand is presented, based on formation enthalpy and cluster geometry.

1. Introduction

Dust grains produced in different tokamaks during normal and off-normal operations are characterized in shape, size and composition by routine procedures [1–7]. Studies performed by optical and scanning electron microscopy have revealed the presence of grains of irregular shape, of count median diameters, roughly speaking of 0.5–20 μm. Recent analyses have shown that deposits collected on the leading edge of the graphitic neutralizers of Tore Supra and TEXTOR are composed of carbon tips in the micrometer size range [8]. By means of high resolution electron microscopy (HRTEM), further investigations have evidenced that in the case of Tore Supra dust samples, these ones contain spherical particulates of 10–70 nm size, of onion-like texture. These particulates are also present in TEXTOR deposits but mixed with carbon of lamellar texture [8]. These results show clearly that nanoparticles can be created by homogeneous nucleation in tokamak plasmas from eroded materials. Previous papers also reported on the existence of very small particles, originating through aerosol nucleation [5,7].

In tokamaks with graphite plasma facing components (PFCs), two sources of production of nanoparticles may operate during normal operations. The precursors can be formed by: (1) condensation of supersaturated carbon vapours originating from the physical erosion of the PFCs, followed by a stage of coagulation of the formed carbon clusters, and (2) through collisions between certain hydrocarbon radicals originating from the chemical erosion of the PFCs. Examples of both routes have already been identified in laboratory experiments with various experimental conditions. For instance, in the case of nanoparticles generated in hydrocarbon discharges with low input power, mass spectrometry showed that positive and negative ions may participate as precursors in the initial stage of dust formation [9]. Taking advantage of these results, a complex precursor growth model was developed [10]. When, the discharge input power is greater, the discharge gas temperature increases and negative ions are no longer stable. In such a case, infrared absorption spectroscopy identified the presence of certain neutral hydrocarbon molecules [11] which may play a role as precursors. A complex thermochemical model of dust nucleation was developed based on these observations [12].

Our study concerns the formation of nanoparticles in a carbon vapor introduced in glow plasmas from cathode sputtering. In such conditions, a first model of precursor formation by coagulation of neutral clusters and of neutral-negative clusters is presented. Experimentally, we have established a scaling law of growth of nanoparticles collected in the glow discharges as a function of the plasma duration. By means of HRTEM, we have observed two successive stages of agglomeration, concomitant to carbon deposition. The agglomeration process favored by surface charge fluctuations stops when the final particles become negatively charged. Hence, we have also observed a growth phase corresponding to cluster deposition occurring when the nanoparticles are negatively charged [13].

2. Experimental conditions

The experiments are performed in argon DC glow discharges between two parallel electrodes as previously described [13]. The electrodes are 10 cm in diameter and separated by 10 cm. The argon pressure is P_g = 0.6 mbar. The discharge current is I_D = 0.08 A.

* Corresponding author.
E-mail address: cecile.arnas@univ-provence.fr (C. Arnas).

0022-3115/$ - see front matter © 2009 Elsevier B.V. All rights reserved.
doi:10.1016/j.jnucmat.2009.01.148

Over 9 min duration, the bias of the graphite cathode varies from −540 V to −580 V. Emission spectroscopy shows that during 9 min, the intensity of argon lines remains rather constant as well as the intensity of C lines and C_2 molecular bands. At $t \sim 9$ min, thermocouples provide the cathode (anode) temperature, $T \sim 120$ °C (~37 °C). In such conditions, the cathode fall length is ~3 mm and the negative glow length (NG) is 7–8 cm as predicted by our simulations. In addition, we find in the NG a mean electron density of $\sim 10^{11}$ cm^3 for an electron temperature of 2 eV. The experimental results presented here were obtained in these stable conditions. For $t > 9$ min, the discharge voltage increases rapidly for reasons that are not reported on here.

3. Modeling of molecular precursors

Carbon clustering in the DC discharges considered in this work starts with the sputtering of the graphite cathode by argon ions. The ion flux and energy are given by a semi-analytical model distinguishing four discharge regions: the sheath, the negative glow, the Faraday dark space (FDS) and the positive column (PC). The sheath is described with a non local model treated by Monte Carlo (MC) simulations that accounts for the conservation of electron flux and energy and for the coupling between the electric field and the electrical charges. The MC simulation is also used to describe the non local ionization which takes place in the NG [14]. The discharge model used for the NG and the FDS allows predicting the electric field reversal at two positions, located at the junction of the sheath and the NG and of the FDS and the PC [15,16]. We have considered that the carbon clusters formed in the discharge as a result of the sputtering process have no effect on the discharge behavior.

The growth model takes into account the formation of neutral and negative clusters. Positive clusters are not considered since such species likely undergo a fast drift toward the cathode. We use the model of Bernholc and Phillips [17] to describe the cluster coagulation where the growth is based on the formation enthalpy and on the cluster geometry. In this model, we consider the coagulation pathway: $C_n + C_x^q \rightarrow C_{n+x}^q$, where $q = 0, -1$ and $x = 1, 2, 3$. The rate constants are determined assuming that each aggregating cluster grows by one carbon atom addition. Hence, the growth starts by the interaction between one carbon atom of a cluster and one given carbon atom of the other cluster [17]. As proposed by Schweigert et al., for a given n, all the possible isomers are considered (chains, mono-cycle, poly-cycle) [18]. A similar rule is adopted for the molecular growth of negative clusters [17]. The charged cluster originates from electron attachment. The charge transfer between neutral and negative clusters is taken into account and significantly affects the relative predominance of negative and neutral clusters. The diffusion and mobility coefficients are estimated from [19]. The equations are time-integrated in a 1D geometry, to determine the axial profile of the different cluster densities. The largest molecular edifice is set for the moment to 30. It is shown that the negative clusters grow in the glow region of the reversed electric field.

Fig. 1 shows the distributions of both neutral and negative clusters at 1 cm above the cathode. The small size domains $n \leqslant 10$ correspond to molecular chains. For larger sizes, the distributions depend strongly on the isomer geometry. A predominance of the neutral clusters is obtained for $n \leqslant 3$, followed by an exponential decrease, up to $n = 10$. Magic numbers with $n = 4m + 3$ periodicity are evidenced from $m = 2$. However, for $n \geqslant 3$ the neutral population is dominated by the negative clusters exhibiting odd magic numbers.

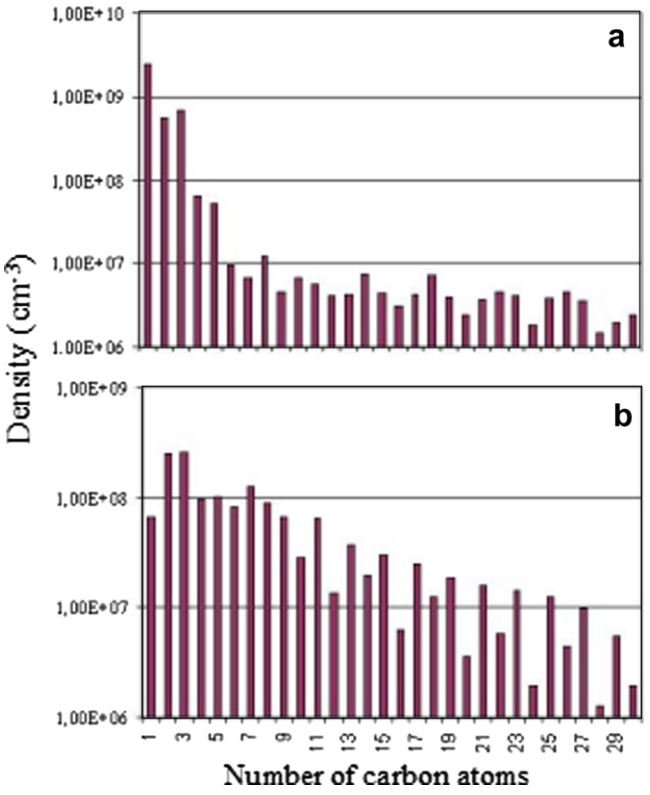

Fig. 1. Distributions of neutral (a) and negative clusters (b). The small size domains $C_{n<10}$ correspond to molecular chains. For larger sizes, the distributions depend strongly on the isomer geometry. The presence of magic numbers is well evidenced.

4. Experimental results

SEM micrographs show that the solid particulates have a spheroid shape. For a given discharge time, the sizes were measured on a large number of particulates in different SEM micrographs of same magnification. The size distributions are lognormal.

Fig. 2 presents the nanoparticle diameter (nm) as a function of the discharge time, $t = 30$, 45, 60, 90, 120, 180, 300 and 540 s. The dots give the mean diameter. The intervals of measurement which cover 68.3% of the total dispersion are established with a multiplicative standard deviation of 1.2. The HRTEM analyses show that in the early stage of growth, nuclei of 2–3 nm size agglomerate to give rise to primary particles (PP) of 5–15 nm size. Fig. 3(a) displays an example, obtained at $t = 60$ s where a PP of ~ 8 nm is formed by two nuclei, welded by carbon deposition. The PPs agglomerate in their turn to form bigger particulates. This is well evidenced in Fig. 3(b) where dust of 45 nm mean size, obtained at $t = 120$ s, is formed by PPs of 5–15 nm size. For $t > 120$ s, the multi-stage agglomeration process is stopped and the growth goes on by cluster deposition with a 2.2 nm/min rate [13].

5. Discussion

A growth phase by successive agglomeration has been evidenced. This mode of growth has already been observed in particulates forming silane plasmas [20]. The origin is attributed to charge fluctuations, leading to positively and negatively charged particulates, favoring Coulomb attraction. Positive surface charge may be due to secondary electron emission (SE) [21,22] which added to ion influx can balance or overcome the electron influx. SE can be produced by the ionizing energetic electrons, accelerated in the cathode fall. In the negative glow where dust is formed, they

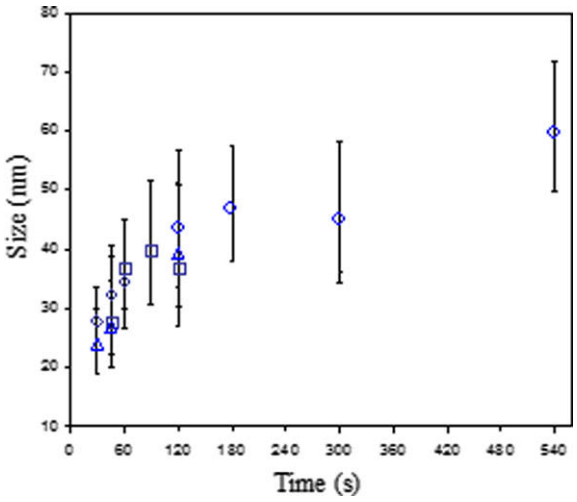

Fig. 2. Scaling law of growth – dust size increase (nm) as a function of the discharge time, t = 30, 45, 60, 90, 120, 180, 300 and 540 s.

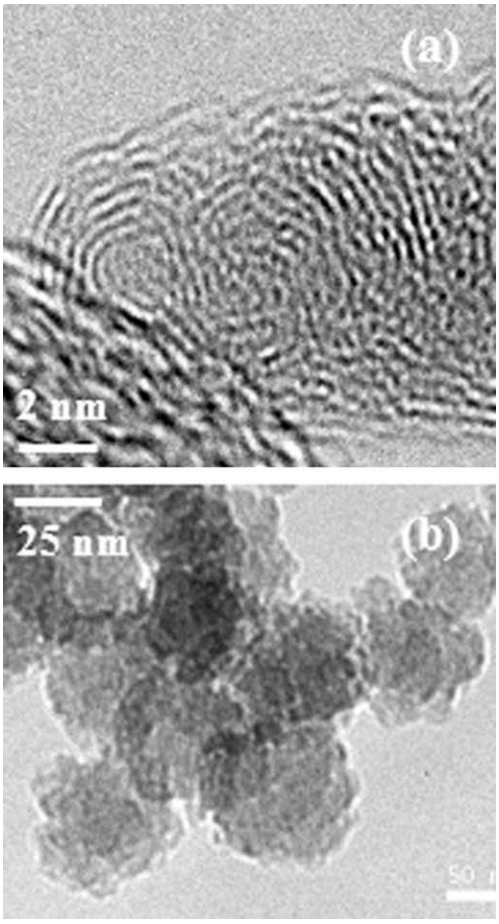

Fig. 3. (a) HRTEM micrograph showing a nanoparticle of ~8 nm size, formed at t = 60 s by two nuclei of 2–3 nm size, welded by carbon deposition, and (b) TEM micrograph showing particulates of 45 nm mean size, formed during 180 s by agglomeration of nanoparticles of 8–10 nm size.

may have enough energy to induce SE. UV radiation emission has also to be considered [22]. In our case, an UV line of 4.2 eV is observed. This energy is slightly lower than the graphite work function of 4.7 eV but may be enough for SE emission in the case of amorphous carbon (a-C) and of carbon containing structural defects. Both features are present in the particles formed at t < 120 s. Indeed, HRTEM show the presence of a-C composed of tetra-coordinated carbon (sp^3 hybridization) and tri-coordinated carbon in the form of isolated aromatic rings (sp^2 hybridization). Structural defects can also be present in a-C as dangling bonds, as bond angles and lengths which are slightly different of sp^2 and sp^3 hybridizations conformations. For instance, Fig. 3(a) shows nuclei with a-C cores and in the periphery, basic structural units (BSUs) formed by concentrically oriented polyaromatic layers [23]. All around, the carbon deposition presents BSUs of ~1 nm length with structural defects in the junction regions. The overall structure could favor SE under UV radiation.

Beyond a given size, the SE added to the ion influx cannot balance anymore the electron influx. The dust charge becomes negative and the agglomeration process is stopped. In such conditions, nanoparticles may grow by carbon cluster deposition.

6. Conclusion

We have presented a study of carbon nanoparticles formation in glow discharges where the carbon source is the sputtered discharge graphite cathode. We have established a first model of growth of dust precursors by coagulation of neutral clusters and of neutral-negative clusters, based on the formation enthalpy and on the cluster geometry. Experimentally, two successive stages of growth of concomitant agglomeration and carbon deposition are observed. The first one concerns the agglomeration of nuclei of 2–3 nm, giving rise to bigger particles which participate to further agglomeration. The growth model by agglomeration of solid particles having charge fluctuations is in progress. In the time interval where the glow plasmas are stable, we have also observed a final growth stage by cluster deposition occurring when the nanoparticles are negatively charged.

Acknowledgements

This work is partially supported by a EURATOM contract in the framework of the Fédération de Recherche Fusion par Confinement Magnétique and partially supported by ANR (Contract No. JC05-42075).

References

[1] W.J. Carmack, K.A. McCarthy, D.A. Petti, A.G. Kellman, C.P.C. Wong, Fus. Eng. Des. 39&40 (1998) 477.
[2] K.A. McCarthy, D.A. Petti, W.J. Carmack, G.R. Smolik, Fus. Eng. Des. 42 (1998) 45.
[3] S.V. Gorman, W.J. Carmack, P.B. Hembree, Fus. Technol. 34 (1998) 745.
[4] A.T. Peacock, P. Andrew, P. Cetier, J.P. Coad, G. Federici, F.H. Hurd, M.A. Pick, C.H. Wu, J. Nucl. Mater. 266–269 (1999) 423.
[5] Ph. Chappuis, E. Tsitrone, M. Mayne, X. Armand, H. Linke, H. Bolt, D. Petti, J.P. Sharpe, J. Nucl. Mater. 290–293 (2001) 245.
[6] S. Muto, T. Tanabe, A. Hirota, M. Rubel, V. Phillips, T. Maruyama, J. Nucl. Mater. 307–311 (2002) 1289.
[7] J.P. Sarpe, V. Rohde, ASDEX-Upgrade Experiment Team, A. Sagara, H. Suzuki, A. Komori, O. Motojima, LHD Experimental Group, J. Nucl. Mater. 313–316 (2003) 455.
[8] M. Richou, C. Martin, P. Delhaès, M. Couzi, C. Brosset, B. Pégourié, A. Litnovsky, V. Phillips, P. Wienhold, J. Dentzer, C. Vix-Guterl, P. Roubin, Carbon 45 (2007) 2723.
[9] Ch. Deschenaux, A. Affolter, D. Magni, Ch. Hollenstein, P. Fayet, J. Phys. D 32 (1999) 1876.
[10] K. de Bleecker, A. Bogaerts, Phys. Rev. E 73 (2006) 026405.
[11] G. Lombardi, K. Hassouni, F. Bénédic, F. Mohasseb, J. Röpcke, A. Gicquel, J. Appl. Phys. 96 (2004) 6739.
[12] K. Hassouni, F. Mohasseb, F. Bénédic, G. Lombardi, A. Gicquel, Pure Appl. Chem. 78 (2006) 1127.
[13] C. Dominique, C. Arnas, J. Appl. Phys. 101 (2007) 123304.
[14] Yuri P. Raizer, in: J.E. Allen (Ed.), Gas Discharge Physics, Springer-Verlag, 1991.
[15] J.P. Boeuf, L.C. Pitchford, J. Phys. D: Appl. Phys. 28 (1995) 2083.
[16] V.I. Kolobov, L.D. Tsendin, Phys. Rev. A 46 (1992) 7837.
[17] J. Bernholc, J.C. Phillips, Phys. Rev. B 33 (1986) 7395.

[18] V. Schweigert, A. Alexandrov, Y. Morokov, V. Bedanov, Chem. Phys. Lett. 235 (1995) 221.
[19] N. Gotts et al., IJMS & Ion Process, 149&150 (1995) 217.
[20] A. Bouchoule, L. Boufendi, Plasma Source Sci. Technol. 2 (1993) 204.
[21] B. Walch, M. Horanyi, S. Robertson, Phys. Rev. Lett. 75 (1995) 838.
[22] U. Kortshagen, U. Bhandarkar, Phys. Rev. E 60 (1998) 887.
[23] A. Galvez, N. Herlin-Boime, C. Reynaud, C. Clinard, J.N. Rouzaud, Carbon 40 (2002) 2775.